Thermochimica Acta 503–504 (2010) 8–11

Contents lists available at ScienceDirect

Thermochimica Acta

journal homepage: www.elsevier.com/locate/tca

Simulation of crystallization sequence during the evaporation of Chott El Jerid brine (south Tunisia)

S. Attia-Essaies [a,*], L. Zayani [a], D. Ben Hassen Chehimi [a], R. Cohen Adad [c], N. Kbir Ariguib [b], M. Trabelsi-Ayadi [a]

[a] Laboratoire d'Applications de la Chimie aux Ressources et Substances Naturelles et à l'Environnement, Faculté des Sciences de Bizerte, 7021 Zarzouna, Tunis 2087, Tunisia
[b] INRST, BP. 95 Hammam Lif 2050, Tunisia
[c] Laboratoire de chimie minérale, 2 Villeurbanne, Lyon, France

ARTICLE INFO

Article history:
Received 19 November 2009
Received in revised form 19 January 2010
Accepted 14 February 2010
Available online 20 February 2010

Keywords:
Solubility diagram
Phase equilibrium
Salts crystallization
Brine evaporation
Quinary system

ABSTRACT

The experimental determination of the brine crystallization sequence during isothermal evaporation is very time consuming. It requires a lot of difficult, tedious, lengthy and inaccurate analyses of liquid and solid phases. However if the phase diagram is known for a given system, application of the geometrical principles of phase rule allows to calculate equilibrium states and to attempt a more easy and accurate determination of the crystallization sequence of natural brine. This method was employed to simulate brine evaporation from Chott El Jerid (Tunisia) at 25 °C and to foresee the solid phases deposed during the process.

1. Introduction

The south of Tunisia contains many mineral reserves of natural brines which are useful for industry and agriculture. These area reserves are called sebkhat or chott. The natural brines are a very complex solubility system, as it includes an important number of ions. The major ions to be considered are Na^+, K^+, Mg^{2+}, Cl^- and SO_4^{2-} in H_2O; and they form a reciprocal quinary system [1–3].

Among the most famous Tunisian salt lakes, Chott El Jerid, in the south, is appearing as the biggest one. It covers 5000 km^2 and contains a total stock of brine estimated to be 5 billion m^3. Its salinity average is 330 g L^{-1}. Chott El Jerid seems to be interesting because of its potassium sulphate content that plays an important role in agriculture.

The objective of this work is to predict the sequence of crystallization of Chott El Jerid brine at 25 °C and under atmospheric pressure based on the phase diagram of the quinary system Na^+, K^+, Mg^{2+}/Cl^-, SO_4^{2-}–H_2O [4].

The calculation is performed assuming that the solids are separated from liquid by sedimentation and no redissolution is possible. The seasonal or day–night fluctuations of temperature and metastable equilibrium have not been taken into account or kinetic crystallization competitive [2,3,5–8].

2. Graphical representation of natural brine

An unsymmetrical expression of composition is desirable in order to get a suitable representation of diagram brines. For the reasons, the Jänecke expression [9] has been found more convenient than the usual expressions (mol fraction, molality, etc.) and has been used in this work. The composition is related to the total amount of anions or cations, taking in account their charge:

$$X_i = \frac{100 z_i n_i}{D}; \quad Y_j = \frac{100 z_j n_j}{D}; \quad Z_H = \frac{100 n_H}{D};$$

$$D = \sum_i z_i n_i = \sum_j z_j n_j \tag{1}$$

In Eq. (1), i and j are related, respectively, to all cations and anions and H to water, n and z are, respectively, the amount and charge of a component; D is the moles number of the solution extended over all anions or cations, taking into account their charge in order to satisfy the electroneutrality condition of the solution.

Under isobaric–isothermal conditions, the brine quinary system involves four composition variables (X_K, X_M, Y_S, Z_H), and its graphical representation requires, in a three-dimensional space, two graphs, one for salt composition and one for the water content.

* Corresponding author.
E-mail address: attiasameh@gmail.com (S. Attia-Essaies).

0040-6031/$ – see front matter © 2010 Elsevier B.V. All rights reserved.
doi:10.1016/j.tca.2010.02.011

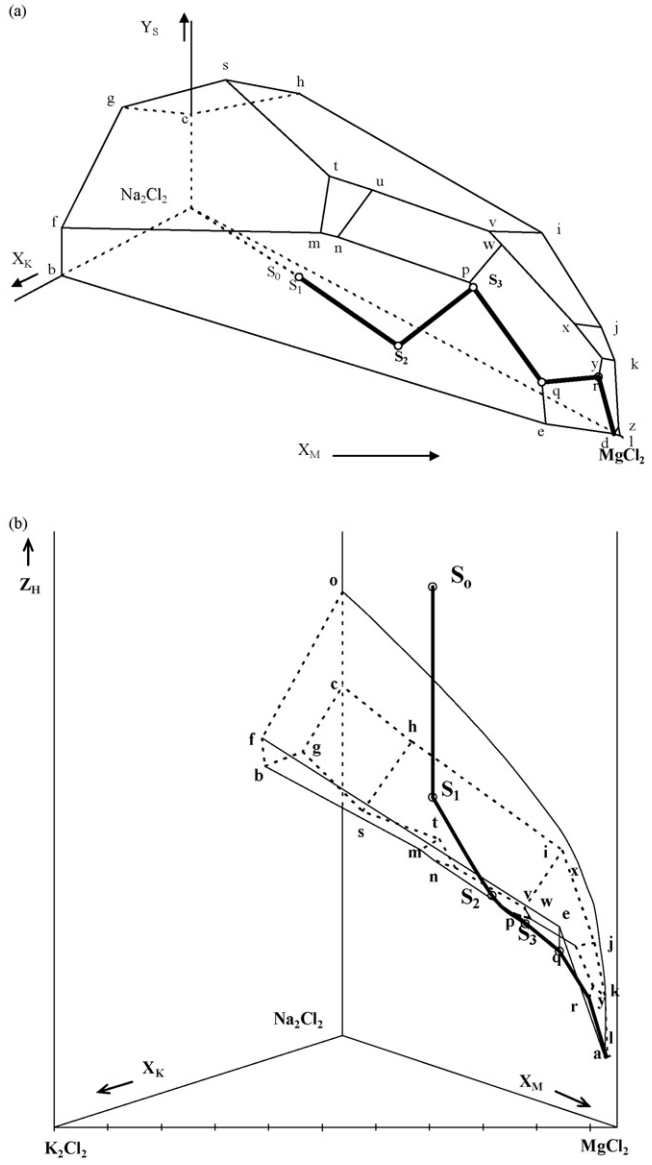

Fig. 1. (a) General sequence of crystallization of brine of Chott El Jerid: salts composition. (b) General sequence of crystallization of brine of Chott El Jerid: water content.

The solubility field of NaCl at 25 °C [2,3,10] (Fig. 1a and b) is limited by 15 faces where a second solid phase co-precipitated with NaCl, 30 monovariante lines of co-precipitation of NaCl with two other salts and 25 invariant points where four solid phases are in equilibrium with saturated solution. The chemical formula, name, symbol, and crystallization field of all solid phases co-precipiting with NaCl at 25 °C are presented in Table 1 [11–27]. The coordinates of invariant points and the observed solid phases are given in Table 2 [3].

3. Geometrical determination of the crystallization sequence

In the determination of the crystallization sequence, the faces of the NaCl solubility field are considered as planes and edges as straight lines. The crystallization sequence is determined by successive step, each phase change corresponding to the end of a step and to the beginning of the next one.

Table 1
Quinary system field of NaCl at 25 °C: chemical formula, name, symbol, and crystallization field of all solid phases co-precipiting with NaCl.

Formula	Name	Symbol	Crystallization field
H_2O	Water	H	
NaCl	Halite	NC	
KCl	Sylvinite	KC	fmnpqeb
$MgCl_2{\cdot}6H_2O$	Bichoffite	MC6	zlad
$KCl{\cdot}MgCl_2{\cdot}6H_2O$	Carnallite	KMC6	qrdze
Na_2SO_4	Thenardite	NS	chgs
$MgSO_4{\cdot}6H_2O$	Hexahydrite	MS6	jkyx
$MgSO_4{\cdot}4H_2O$	Leonhardite	MS4	ykldr
$MgSO_4{\cdot}7H_2O$	Epsomite	MS7	vijxw
$Na_2SO_4{\cdot}3K_2SO_4$	Glaserite	N3KS	fgstm
$Na_2SO_4{\cdot}MgSO_4{\cdot}4H_2O$	Astrakanite	NMS4	shivut
$K_2SO_4{\cdot}MgSO_4{\cdot}6H_2O$	Schoenite	KMS6	tumn
$K_2SO_4{\cdot}MgSO_4{\cdot}4H_2O$	Leonite	KMS4	uvwpn
$KCl{\cdot}MgSO_4{\cdot}3H_2O$	Kainite	KCMS3	wxyrpq

The mean composition of salts remains constant during each step so that the relative amounts of salts distributed between the phases in equilibrium can be evaluated by application of the lever rule.

The number of steps of crystallization sequence depends on the initial composition of the brine. In the case of the brine of Chott El Jérid, the crystallization sequence involves six steps.

3.1. First step: saturation of the brine with NaCl

Starting point $S_0(X_K^0, X_N^0, X_M^0, Y_S^0, Z_H^0)$; end point $S_1(X_K^1, X_N^1, X_M^1, Y_S^1, Z_H^1)$.

The initial composition of the brine of Chott el Jerid is inside the NaCl solubility field, but water content is outside since the solution is dilute (S_0 in Fig. 1a).

During the evaporation the water content decreases without change of salt composition until the solution becomes saturated in sodium chloride.

The water amount cannot be directly determined at the end of this step, i.e. when the solution is just saturated in NaCl.

Table 2
Solubility of NaCl at 25 °C: invariant points.

Point	X_K	X_M	Y_S	Z_H	Equilibrium solid phase
c	0.00	0.00	20.21	802	NC + NS
g	14.71	0.00	21.80	722	NC + NS + N3KS
h	0.00	25.29	28.90	762	NC + NMS4 + NS
s	14.25	22.15	30.72	694	NC + NS + NMS4 + N3KS
t	14.38	47.94	25.34	685	NC + NMS4 + N3KS + KMS6
u	13.96	56.52	25.85	663	NC + NMS4 + KMS6 + KMS4
v	9.01	77.47	24.65	628	NC + NMS4 + KMS4 + MS7
w	9.04	79.85	24.20	619	NC + MS7 + KMS4 + KCMS3
i	0.00	81.79	23.55	682	NC + NMS4 + MS7
f	29.68	0.00	6.95	738	NC + N3KS + KC
m	19.37	49.06	19.38	678	NC + N3KS + KMS6 + KC
n	18.62	52.93	19.50	669	NC + KMS6 + KC + KMS4
p	11.38	75.89	18.31	623	NC + KC + KMS4 + KCMS3
x	4.28	91.69	15.15	595	NC + MS7 + MS6 + KCMS3
j	0.00	94.64	14.25	596	NC + MS7 + MS6
q	7.00	88.32	6.30	598	NC + KC + KCMS3 + KMC6
z	0.34	99.02	1.04	475	NC + MC6 + MS1 + KMC6
l	0.00	99.10	1.25	476	NC + MC6 + MS1
a	0.00	99.25	0.00	480	NC + MC6
e	6.91	88.04	0.00	615	NC + KMC6 + KC
b	30.20	0.00	0.00	770	NC + KC
k	0.00	96.95	10.06	540	NC + MS6 + MS1
y	2.21	96.13	11.05	552	NC + MS6 + KCMS3 + MS1
r	2.25	95.31	8.08	539	NC + KCMS3 + KMC6 + MS1
d	0.41	98.84	0.00	478	NC + KMC6 + MC6

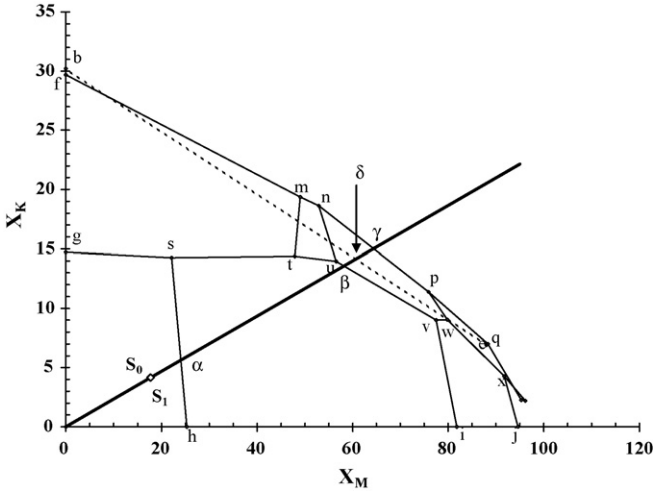

Fig. 2. Projection on the basic plane (X_K, X_M) of the solubility domain of NaCl, Intersection between (O, S_1) and the solubility domain of NaCl.

3.2. Second step: precipitation of NaCl

Starting point $S_1(X_K^1, X_N^1, X_M^1, Y_S^1, Z_H^1)$; end point $S_2(X_K^2, X_N^2, X_M^2, Y_S^2, Z_H^2)$.

The second step of evaporation corresponds to the precipitation of NaCl. According to the lever rule, the representative point of the salt composition moves along the line NaCl-S_1. This line has the equation:

$$\frac{X_K}{4.15} = \frac{X_M}{17.75} = \frac{Y_S}{2.23} \tag{2}$$

A second solid phase appears when the representative point of the solution reaches a face of the solubility field of NaCl (point S_2) the calculation of S_2 coordinates are determined in two steps:

(i) The intersection between the vertical plane OS_1 and the solubility field of NaCl is deduced from the horizontal projections of OS_1 and the NaCl solubility field on the base of the representative prism (Fig. 2). The plane cuts the NaCl domain on edges sh, uv, np and be respectively on the points α, β, γ and δ.

The coordinates of point α, for example, are obtained by solving these two equations: The equation for the edges (s, h):

$$\frac{X_{K\alpha} - X_{Kh}}{X_{Ks} - X_{Kh}} = \frac{X_{M\alpha} - X_{Mh}}{X_{MS} - X_{Mh}} = \frac{Y_{s\alpha} - Y_{sh}}{Y_{ss} - Y_{sh}} \tag{3}$$

and the equation of the line (O, S_1):

$$\frac{X_{K\alpha} - X_{K0}}{X_{KS_1} - X_{K0}} = \frac{X_{M\alpha} - X_{M0}}{X_{MS_1} - X_{M0}} \tag{4}$$

The same approach is followed to determine the coordinates of other points β, γ, δ (Table 3).

(ii) The vertical planes (o, c, α, β, γ, δ) (Fig. 3a) reveal that the point S_2 is located between γ and δ. It corresponds to a double saturation in NaCl and KCl and its coordinates are given by intersect of (O, S_1) and (γ, δ) (Fig. 3b).

Table 3
Coordinates of intersections in the field of crystallization NaCl with the edge (OS_1).

Points	Coordinates of Jänecke			
	X_K	X_M	Y_S	Z_H
α	6.20	26.65	29.69	739
β	13.56	58.21	24.23	619
γ	15.00	64.39	18.90	646
δ	14.14	60.70	0.00	663

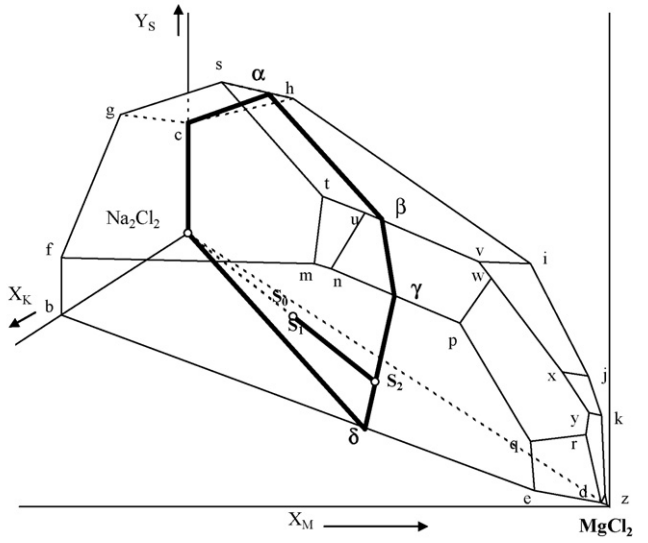

Fig. 3. Intersection between the vertical plane (o, c, α, β, γ, δ) and (O, S_1).

The coordinates of point S_2 are obtained by solving these two equations:

The equation of the line (O, S_1):

$$\frac{X_{KS_2}}{X_{KS_1}} = \frac{X_{MS_2}}{X_{MS_1}} \tag{5}$$

The equation for the edge (γ, δ):

$$\frac{X_{KS_2} - X_{K\gamma}}{X_{K\gamma} - X_{K\delta}} = \frac{X_{MS_2} - X_{M\gamma}}{X_{M\gamma} - X_{M\delta}} \tag{6}$$

The analytic expression of crystallization field of NaCl was determined from a semi-empirical model for modeling the equilibrium diagram of the quinary system Na^+, K^+, Mg^{2+}/Cl^-, SO_4^{2-}–H_2O [2].

$$Z_H = p(X_N Y_C)^{1/2} \exp(qX_M) - 200 + \left(\frac{Y_S + X_M}{2}\right) \tag{7}$$

The parameters p and q in this expression are adjustable. They may be calculated from the coordinates of two points belonging to the solubility field of NaCl. In the frame of this work, the two points considerate are the S_2 and O (solubility of NaCl in binary system NaCl–H_2O at 25 °C) [4].

At this stage, the water amount of S_1 can be determined (Z_H^1 = 880).

3.3. Third step: co-precipitation of NC and KC

Starting point $S_2(X_K^2, X_N^2, X_M^2, Y_S^2, Z_H^2)$; end point $S_3(X_K^3, X_N^3, X_M^3, Y_S^3, Z_H^3)$.

During co-crystallization of NaCl and KCl, the representative point of saturated solution moving along the line S_2–S_3 (S_3 is the intersection between the limiting face of the solubility field of NaCl (face bfmnpqe) and the plane defined by S_2), NaCl and KCl. A projection of the field of solubility of NaCl in the plane (NC, X_M, Y_S) shows that the edge (O, S_2) crosses the monovariante line (p, q), which represents the three salts co-precipitation NC, KC, and Kaïnite $KClMgSO_4{\cdot}3H_2O$ (Fig. 4).

At this step the coordinates of S_3 are determined.

3.4. Fourth step: co-precipitation of NC, KC and KCMS3

Starting point $S_3(X_K^3, X_N^3, X_M^3, Y_S^3, Z_H^3)$; end point q($X_K^q, X_N^q, X_M^q, Y_S^q, Z_H^q$).

Table 4
Coordinates of end and the starting points as well as the salts deposited during each stage.

Steps	Point	Start				End				Deposed salts
		X_K	X_M	Y_S	Z_H	X_K	X_M	Y_S	Z_H	
1	S_0–S_1	4.15	17.75	4.14	960	4.15	17.75	4.14	880	
2	S_1–S_2	4.15	17.75	4.14	880	14.80	63.52	14.63	650	NC
3	S_2–S_3	14.80	63.52	14.63	650	11.16	76.51	17.67	646	NC + KC
4	S_3–q	11.16	76.51	17.67	646	7.00	88.32	6.30	598	NC + KC + KCMS3
5	q–r	7.00	88.32	6.30	598	2.25	95.31	8.08	539	NC + KCMS3 + KMC6
6	r–d	2.25	95.31	8.08	539	0.34	99.02	1.04	475	NC + KMC6 + MS4

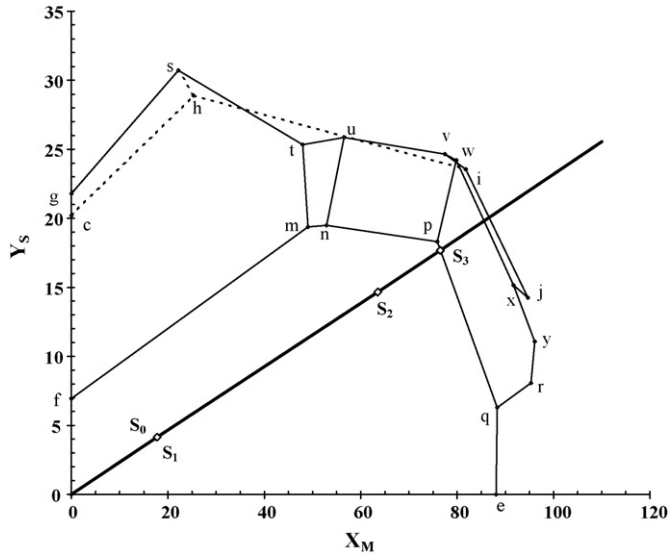

Fig. 4. Projection of the saline composition in the (NC, X_M, Y_S). Intersection of the field of crystallization of NaCl with right (O, S_2).

During the fourth step three salts, NaCl, KCl and $KClMgSO_4{\cdot}3H_2O$ are in equilibrium with the liquid. The paths of brine move along the edges (p, q). The representative point of saturated solution S_4 is merged with q. The fourth salt observed during evaporation of the brine is KMC6 (Carnallite). In this point the variance is zero and brine leaves this point with the disappearance of one of phases.

3.5. Fifth step: co-precipitation of NC, KCMS3 and KMC6

Starting point q($X_K^q, X_N^q, X_M^q, Y_S^q, Z_H^q$); end point r($X_K^r, X_N^r, X_M^r, Y_S^r, Z_H^r$).

During evaporation of the brine water quantity is decreasing continuously. Indeed, the representative point of the solution evolves to the point where the water is lowest.

Based on bibliographic data the brine evolves to the point r and the solid phase that was lost before leaving the point q is sylvinite and the fourth salt observed in the point r is KMC6.

The representative point of saturated solution leaves the point r when the salt $KClMgSO_4{\cdot}3H_2O$ disappears.

3.6. Sixth step: co-precipitation of NC, KMC6 and MC6

Starting point r($X_K^r, X_N^r, X_M^r, Y_S^r, Z_H^r$); end point d($X_K^d, X_N^d, X_M^d, Y_S^d, Z_H^d$).

The representative point of saturated solution moves along the edges (r, d). On this edge there is co-precipitation of halite, carnallite and léohardite appears when the representative point of saturated solution reaches the point r.

Fig. 1a and b shows a general sequence of crystallization of brine of Chott El Jerid. Table 4 gathers the coordinates of the end and the starting points as well as the salts deposited during each stage.

4. Conclusion

The present paper demonstrates the steps of calculation and its geometrical counter-part to obtain the crystallization sequence from brine of Chott El Jerid.

Water from this brine is rich in potassium. The second solid phase observed is sylvinite. Among the six salts deposited during the evaporation, three are potassium salts KCl, $KClMgSO_4{\cdot}3H_2O$ and $KClMgCl_2{\cdot}6H_2O$.

References

[1] R. Cohen-Adad, M-Th. Cohen-Adad, D. Chehimi, A. Marrouche, in: J.P. Calliste, A. Truyol, J. Westbrooke (Eds.), Thermodynamic Modeling and Materials Data Engineering, Springer, Berlin, 1998, pp. 95–108.
[2] L. Zayani, Thesis, Tunis University (1999).
[3] R. Cohen-Adad, M-Th. Cohen-Adad, C. Balarew, S. Tepavitcharov, W. Voigt, L. Zayani, D. Ben Hassen-Chehimi, S. Mançour-Billah, Monatshefte für Chemie 131 (2000) 25–37.
[4] R. Cohen-Adad, J.W. Lorimer, Alkali Metal and Ammonium Chloride in Water and Heavy Water, Solubility Data Series, Vol. 47, Pergamon Press, Oxford, 1991.
[5] D. Ben Hassen-Chehimi, M. Trabelsi-Ayadi, N. Kbir-Arigui, R. Cohen-Adad, M-Th. Cohen-Adad, J.E.E.P. XXIII, Tunis, 1997.
[6] R. Cohen-Adad, M-Th. Cohen-Adad, L. Zayani, D. Chehimi, VIII I.S.S.P., Niigata, 1998.
[7] R. Cohen-Adad, D. Ben Hassen-Chehimi, L. Zayani, M-Th. Cohen-Adad, M. Trabelsi-Ayadi, N. Ariguib, Calphad 4 (1997) 521.
[8] R. Cohen-Adad, M-Th. Cohen-Adad, D. Chehimi, L. Zayani, Calphad XXVI, Beijing, 1998.
[9] E. Janecke, Z. Anorg. Chem. 51 (1906) 132.
[10] E. Uskwski, M. Dietzel, Atlas and Data of Solid-Solution Equilibria of Marine Evaporite, Springer, Berlin, 1998.
[11] J. D'Ans, Die Lösungsgleichgewichte der systeme der Salze ozeanisher Salzablagerungen, vols. 1and 2 (tables), Verlagsges. Für Ackerbau M.B.H, Berlin, 1933.
[12] J.H. Van'thoff, W. Meyerhoefer, F.N. Smith, Physik. Math. KI 23 (1901) 1034.
[13] H. Holldorf, N. Menzel, Freinberg-Forschungsh A A960 (1984) 27.
[14] M. Nur'yagdyrv., L.M. Pasev'eva, A.Ch. Elomanova, Izv. Akad. Nauk Turkm. SSR, Fiz. Tekh, Khim. Geol. Nauk 5 (1981) 83.
[15] M. Nur'Yagdyen, G.M. Andriasova, A. Kolatova, Izv. Akad. Nauk Turkm. SSR, Ser. Fiz-Tekh., Khim. Geol. Nauk 2 (1981) 79.
[16] O. Karsten, U. Kali., Steisalz 7 (1979) 445.
[17] H. Emos, E. Schreck, H. Holldorf, Rev. Chem. Min. 11 (1974) 227.
[18] O.K. Yanat'eva., Izvest. Sectora Fiz-Chim. Analiza 17 (1949) 370.
[19] K. Koelichen, mitt. Kali-Forsch. Anst. G.m.b.H. 1 (1919) 15.
[20] C.E. Harvie, J.H. Weare, Geochim. Cosmochim. Acta 44 (1980) 981.
[21] M.G. Valyatchko, E.F. Solov'Eva, Tru. Vses. Nauk. Issled. Inst. Galurgii 21 (1949) 197.
[22] B.P. Choudhari, J. Appl. Chem. Biotechnol. 21 (1971) 266.
[23] H. Autenrieth, Kali u. Steinsalz 1 (1954) 7–13.
[24] H. Autenrieth, Kali u. Steinsalz 1 (1955) 18.
[25] R. Beck, H.H. Emons, H. Holldorf, Freig. Forschungsh a A628 (1982) 19.
[26] Ya.G. Goroshchenko, L. Soliev, V.K. Mardanenko, L.A. Borisenko, Russ. J. Inorg. Chem. 24 (10) (1979) 1568.
[27] P. Hadzeriga, Soc. Mint. Eng. (1964) 169.